The Journal of Physical Chemistry A

 VOLUME 103, NUMBER 42, OCTOBER 21, 1999

ARTICLES

193 nm Photodissociation of Thiophene Probed Using Synchrotron Radiation

Fei Qi, Osman Sorkhabi, Abbas H. Rizvi, and Arthur G. Suits*

Chemical Sciences Division, Ernest Orlando Lawrence Berkeley National Laboratory, Berkeley, California 94720

Received: June 21, 1999; In Final Form: August 23, 1999

The photodissociation dynamics of thiophene, c-C_4H_4S, have been studied at 193 nm using tunable synchrotron undulator radiation as a universal product probe. Five primary dissociation channels have been observed, and the translational energy distributions and photoionization efficiency spectra have been recorded for all products. The evidence suggests that dissociation occurs on the ground-state surface following internal conversion.

I. Introduction

Although detailed photochemical studies of simple molecules have provided considerable insight into the dynamics of elementary chemical reactions, analogous studies for more complex molecules have been less ardently pursued, largely owing to experimental challenges attending such investigations. The availability of a universal, selective vacuum ultraviolet (VUV) probe on the chemical dynamics beamline[1] has recently made possible new approaches to the study of the photodissociation dynamics of large molecules. In this paper, we extend our recent investigations of the photochemistry of complex cyclic molecules[2] to include thiophene, a five-membered sulfur-containing heterocyclic aromatic molecule.

Thiophene is one of the principal sulfur carrying compounds in fossil fuels, and the study of its photodissociation can provide insights into the properties of sulfur-containing molecules and radicals of importance in fossil fuel combustion.[3] The ultraviolet (UV) photochemistry of thiophene was studied in the gas phase at 213.9, 228.8, and 253.7 nm by Wiebe and Heicklen in the late 1960s using end-product analysis.[4] The primary photofragments inferred from the experiments included C_2H_2, $CH_2{=}C{=}CH_2$, $CH_3C{\equiv}CH$, CS_2, $CH_2{=}CH{-}C{\equiv}CH$, and C_2H_2S. Infrared laser multiphoton excitation/dissociation of thiophene was studied by Nayak et al.[5] They proposed a mechanism that involved breakage of the C−S bond in thiophene to form an unstable 1,5-diradical which further decomposed via different channels. Krishnamachari and Venkitachalam observed a transient absorption spectrum in the region 377−417 nm following flash photolysis of thiophene.[6] They tentatively assigned this absorption to C_4H_3. The first direct examination of primary photoproducts of thiophene at 193 nm was carried out by Myers using photofragment translational spectroscopy and reported in his thesis work but not otherwise published.[7] Six primary dissociation channels were identified as discussed below. Ng and co-workers examined the isomeric structures of the primary photoproducts formed in the 193 nm photodissociation of thiophene using photodissociation−photoionization detection of the hydrocarbons and 2 + 1 resonance-enhanced multiphoton ionization (REMPI) detection of the sulfur atom. Only two dissociative channels, $C_2H_2S + C_2H_2$ and $C_4H_4 + S$, were observed in their studies, and they found that the S atoms were produced predominantly (≥ 96%) in the ^3P_J states.[8]

Thiophene is the sulfur-containing analogue of furan, the subject of a recent photodissociation study from our laboratory.[2] A comparison of the behavior of these systems promises insight into the role of issues such as energetics and spin−orbit

* Corresponding author: agsuits@lbl.gov

10.1021/jp992057h CCC: $18.00
Published on Web 09/23/1999

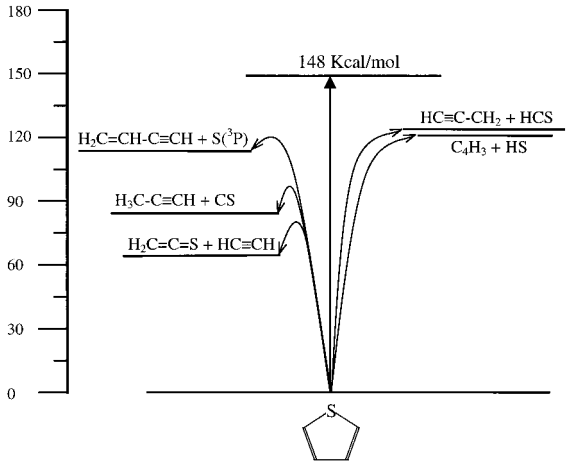

Figure 1. Energy diagram showing all observed product channels from 193 nm dissociation of thiophene, along with barriers estimated from the results.

mediated processes in the photodissociation dynamics of closely related systems. Our study of the photodissociation of furan at 193 nm employed photofragment translational spectroscopy with tunable VUV probe provided by synchrotron radiation, just as in the present thiophene experiments. Three primary channels were observed from furan: HCO + C_3H_3, CO + C_3H_4, and H_2CCO + C_2H_2. The evidence suggested that the two closed-shell channels occur on the ground state potential energy surface (PES) following internal conversion, while the radical channel likely takes place on an excited PES. All channels exhibited a barrier for dissociation with the acetylene + ketene channel having the largest value at about 25 kcal/mol. Angular distribution measurements showed anisotropy only for the radical channel. These findings were found to be consistent with a rapid excited-state dissociation for the radical channel and slow dissociation for the other two pathways.

In this study, we have measured the time-of-flight (TOF) and photoionization efficiency spectra (PIE) of photofragments from the photolysis of thiophene using photofragment translational spectroscopy with synchrotron undulator radiation on the chemical dynamics beamline at the Advanced Light Source. Five primary dissociation channels have been identified, including three closed-shell channels and two radical channels, as summarized below.

$$C_4H_4S\ (\text{thiophene}) + h\nu_{193\ nm} \rightarrow C_4H_4 + S(^3P) \quad (1)$$

$$\rightarrow C_2H_2S + C_2H_2 \quad (2)$$

$$\rightarrow C_3H_4 + CS \quad (3)$$

$$\rightarrow HS + C_4H_3 \quad (4)$$

$$\rightarrow HCS + C_3H_3 \quad (5)$$

Channels analogous to **2**, **3,** and **5** were observed in the dissociation of furan at 193 nm.[2] Two additional channels, **1** and **4,** were observed in the present study. Figure 1 shows the energy diagram of the observed photodissociation pathways for thiophene at 193 nm.

II. Experimental Section

The experiments were performed on beamline 9.0.2.1 of the Advanced Light Source using a rotatable source molecular beam apparatus described in detail elsewhere.[9,1] Helium was bubbled through a thiophene sample held at room temperature. The total pressure was about 800 Torr, thus yielding a 10% mixture of thiophene in He. The mixture was fed through a pulsed valve and expanded from a nozzle heated to ~80 °C into the main chamber. The resulting molecular beam was collimated with two skimmers and its velocity and speed ratio were found to be 1280 ± 10 m/s and 7 ± 1 m/s, respectively. Thiophene (99%) was obtained from Aldrich and used without further purification.

The molecular beam was intersected at 90° with an ArF excimer laser beam. The laser beam was focused to a spot of size 2 × 4 mm and aligned perpendicular to the plane containing the molecular beam and detector axes, on the axis of rotation of the molecular beam source. Photofragments entering the triply differentially pumped detector region were photoionized 15.2 cm downstream from the interaction region using tunable synchrotron radiation. The characteristics of the light source have been discussed in detail elsewhere,[1] but include a flux of 10^{16} photons/s (quasi-continuous), an energy bandwidth of 2.2%, and a cross-section in the probe region of 0.2 × 0.1 mm. The photoionized products were mass selected by a quadrupole mass filter and the ions were counted with a Daly ion counter. Time-of-flight spectra of the neutral products were measured with a multichannel scaler (MCS) whose bin width was fixed at 1 μs for the measurements reported here. Timing sequences for the laser, pulsed valve, and MCS were controlled by a digital delay generator. Eight quartz plates fixed at Brewster's angle were used for the polarization measurements to give 87 ± 5% polarized light. A half-wave plate (Karl Lambrecht) was used to rotate the angle of polarization with respect to the detector axis. Care was taken to ensure that the TOF spectra shown here are free of multiphoton effects (except where indicated).

The tunability of the VUV light source allows measurements of photoionization efficiency (PIE) spectra and for the selective ionization of products with very low background counts. A series of TOF spectra were recorded at a fixed angle for different photoionization energies, then they were normalized for the probe photon flux and integrated to obtain the PIE spectra. A gas filter filled with about 25 Torr of Ar was used to eliminate higher harmonics of the undulator radiation.[10] A MgF_2 optical filter also was used to eliminate small contamination of the probe light by higher energy photons when probing below 10.5 eV.

III. Results and Discussion

TOF spectra of photofragments from photodissociation of thiophene at 193 nm have been measured at several angles from 20° to 50°. Signal at m/e = 58, 52, 51, 45, 44, 40, 39, 33, 32, and 26 were detected. These correspond to C_2H_2S, C_4H_4, C_4H_3, HCS, CS, C_3H_4, C_3H_3, HS, S, and C_2H_2, respectively. In all of the TOF spectra presented here, the open circles represent the experimental data, the dash lines and the dash−dot lines are single channel contributions to the forward convolution fit, and the solid lines are the overall fit to the data. A forward convolution fit to data was used to get total center of mass translational distributions, P(E).[11,12] Although we typically show TOF spectra for only one angle for each product, mutiple angles were recorded and fitted for each channel shown. Figure 1 shows the energy diagram including the five observed primary dissociation channels. Table 1 lists the energetics of the isomers of the various species observed in this study.

Figure 2 shows PIE spectra of the fragment C_4H_4 (a), C_3H_3 (b), C_2H_2S (c), C_3H_4 (d), C_4H_3 (e), and CS (f). The onset in each PIE curve is roughly determined by linear extrapolation. Onsets obtained in this study are also listed in Table 1. We will present the experimental results and data fits according to the approximate relative signal intensity of each dissociation channel.

TABLE 1: Energetics for Isomers of the Observed Fragments

mass detected[a]	neutral species[b]	$\Delta H_{f,298}$ (kcal/mol)[c]	literature IP (eV)[c]	this work (eV)
84 (C_4H_4S)	C_4H_4S (thiophene)	27.5	8.87	
52 (C_4H_4)	$CH_2{=}CH{-}C{\equiv}CH$	73	9.58	9.4
	$CH_2{=}C{=}C{=}CH_2$	83	9.15	
	$C{=}C{-}C{=}CH_2$	101	8.15	
51 (C_4H_3)	$CH{\equiv}C{-}C{=}CH_2$	116[d]		~9.2
	$CH{\equiv}C{-}CH{=}CH$	126[d]		
40 (C_3H_4)	$CH_3{-}C{\equiv}CH$	44.2[e]	10.36[e]	9.6
	$CH_2{=}C{=}CH_2$	45.5[e]	9.69[e]	
	c-C_3H_4	66.2[e]	9.67[e]	
39 (C_3H_3)	$CH{\equiv}C{-}CH_2$	81.1[f]	8.67[g]	8.6
	c-C_3H_3	105[h]	6.6	
58 (C_2H_2S)	$CH_2{=}C{=}S$	39	8.77	8.7
	c-$CH{=}CHS$	≈87[i]	7.4[i]	
	$CH{=}CHS$	≈101[i]		
45 (HCS)	HCS	71.7[j]		
	HSC	111.3[k]		
44 (CS)	CS	67[l]	11.33[e]	
26 (C_2H_2)	$HC{\equiv}CH$	54.4	11.40	
33 (HS)	HS	33.3[l]	10.42[m]	
32(S)	S	66.25 (^3P)[e]	10.36[e]	

[a] Ions observed which are attributable to VUV photoionization of photofragments for thiopheneat 193 nm. [b]Possible isomers for photoproducts of thiophene formed at 193 nm. [c] Heat of formation at 298 K. Values are from ref 13 unless otherwise stated. [d] References 17 and 18. [e] Reference 25. [f] Reference 26. [g] Reference 27. [h] Reference 28. [i] References 8 and 29. [j] Reference 30. [k] References 31 and 16. [l] Reference 32. [m] Reference 33.

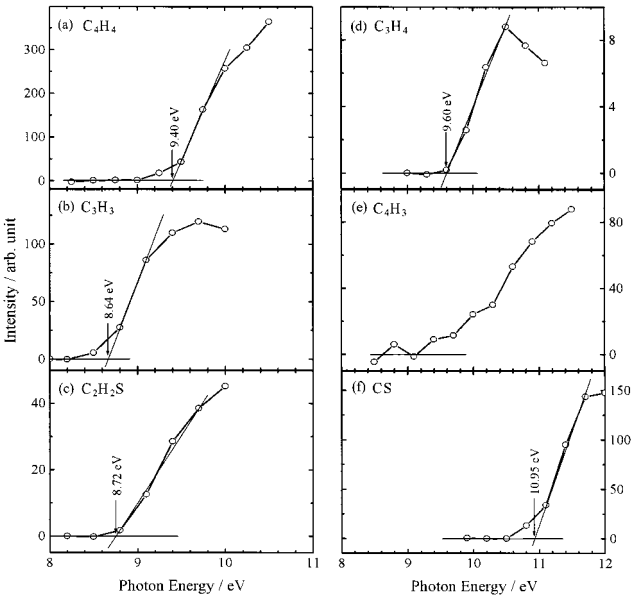

Figure 2. Low-resolution photoionization efficiency spectra for the indicated photoproducts, along with approximate thresholds.

The C_4H_4 + S Channel. TOF spectra of the C_4H_4 and S fragments measured at different angles are shown in Figure 3. The photoionization energy was 11.0 and 10.5 eV, respectively. The contribution of dissociative ionization of larger fragments (C_2H_2S, HCS, CS, and HS) to sulfur atom may be excluded since a MgF_2 window was used to cut off high-energy scattered radiation. However, these contributions were observed using electron impact ionization in Myers' study. The TOF spectra of mass 52 (C_4H_4) were fitted using the translational energy distribution shown where indicated in Figure 4. This P(E) fits all measured angles. The P(E) is peaked at 4 kcal/mol with an average translational energy of 4.9 kcal/mol. This P(E) extends out to about 17 kcal/mol.

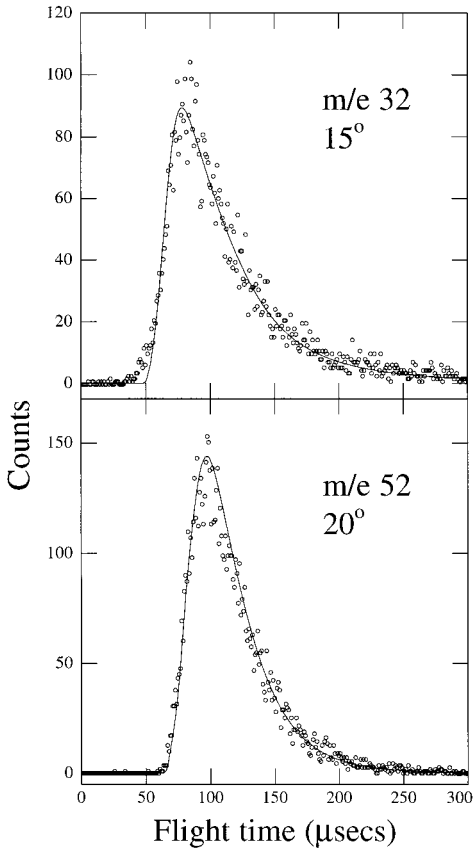

Figure 3. Time-of-flight (TOF) spectra for the C_4H_4 + S channel at 20°.

Depending on the structure of mass 52 (C_4H_4), three possible dissociation channels are allowed energetically.[8] They are

$$C_4H_4S\ (\text{thiophene}) + h\nu_{193\ nm} \rightarrow$$

$$CH_2{=}CH{-}C{\equiv}CH + S(^3P) \quad \Delta H^0_{298} = -36\ \text{kcal/mol} \qquad (1a)$$

$$CH_2{=}C{=}C{=}CH_2 + S(^3P) \quad \Delta H^0_{298} = -26.0\ \text{kcal/mol} \qquad (1b)$$

$$C{=}C{-}C{=}CH_2 + S(^3P) \quad \Delta H^0_{298} = -8.0\ \text{kcal/mol} \qquad (1c)$$

The analogous channel, C_4H_4 + O, was not observed for furan even though the above three dissociation channels were energetically allowed.[2] It is likely that the weaker C−S bond contributes to the observation of these channels for thiophene.

The PIE spectrum for C_4H_4 is shown in Figure 2a. It is clear that the C_4H_4 fragment is produced predominantly as vinyl acetylene ($H_2C{=}CH{-}C{\equiv}CH$). Our assignment is based upon the following considerations. The onset is 9.40 eV labeled by an arrow and is very close to the ionization potential (IP) of vinyl acetylene (9.58 eV).[13] IP for 1,2,3-butatriene ($CH_2{=}C{=}C{=}CH_2$) and methylenecyclopropene ($C{=}C{-}C{=}CH_2$) are 0.25 and 1.25 eV lower than the observed onset, respectively. The latter is thus ruled out as a major contributor to the *m*/*e* 52 product. The formation of 1,2,3-butatriene (process **1b**) is not excluded by our results, but energetic considerations suggest that **1a** is likely to dominate. Finally, the PIE curve drops down slowly at the region of 9.5 to 9.0 eV. The C_4H_4 fragment likely carries some internal energy, causing the observed threshold to shift toward low energies, although not to the full extent of the average internal energy of 31 kcal/mol (1.3 eV). These conclusions are in good agreement with previous studies.[8]

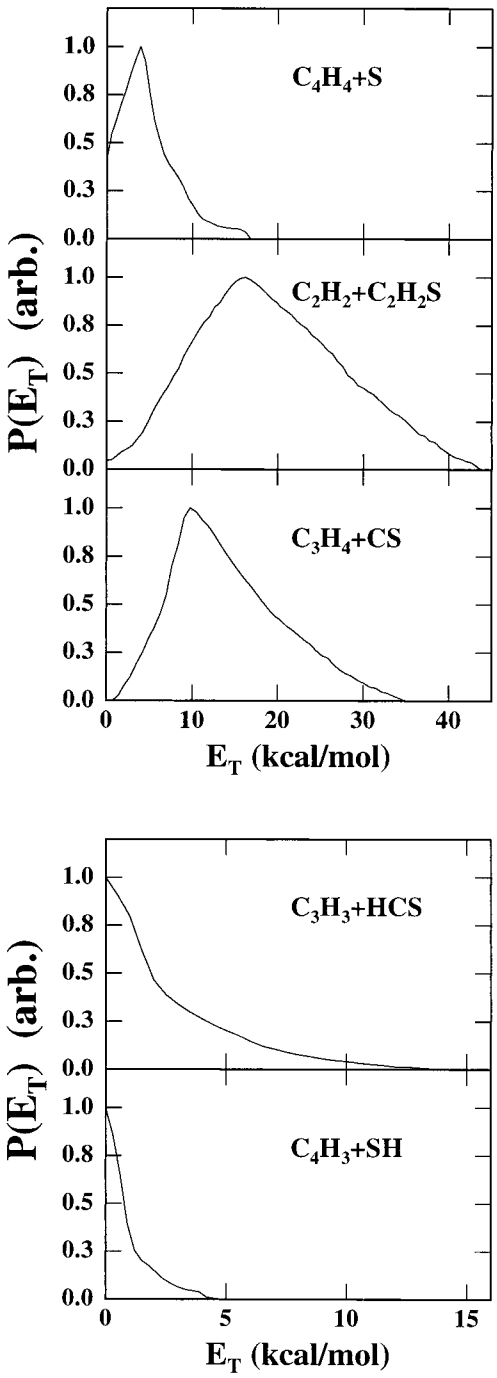

Figure 4. Translational energy distributions (P(E)s) for the indicated product channel.

Angular distribution measurements for this channel yielded an isotropic product angular distribution (i.e., $\beta = 0$), implying that the dissociation process takes place on a time scale longer than several molecular rotation periods.

Since the first excited S (^{1}D) state lies 26.52 kcal/mol above the ground (^{3}P) state,[14] S (^{1}D) can be also formed together with vinyl acetylene in process **1a**. Some evidence for excited S (^{1}D) was observed in this study: that is, S atom product appearing below the IP for S(^{3}P). However, this product was found at translational energies only accessible with multiphoton excitation, leading us to conclude that it is not a product of single photon dissociation of thiophene.

The C_2H_2S + C_2H_2 Channel. TOF spectra of the C_2H_2S and C_2H_2 fragments were measured at 20°, 35°, and 50°, respectively. Photon energies of 10.0 and 12.5 eV were used

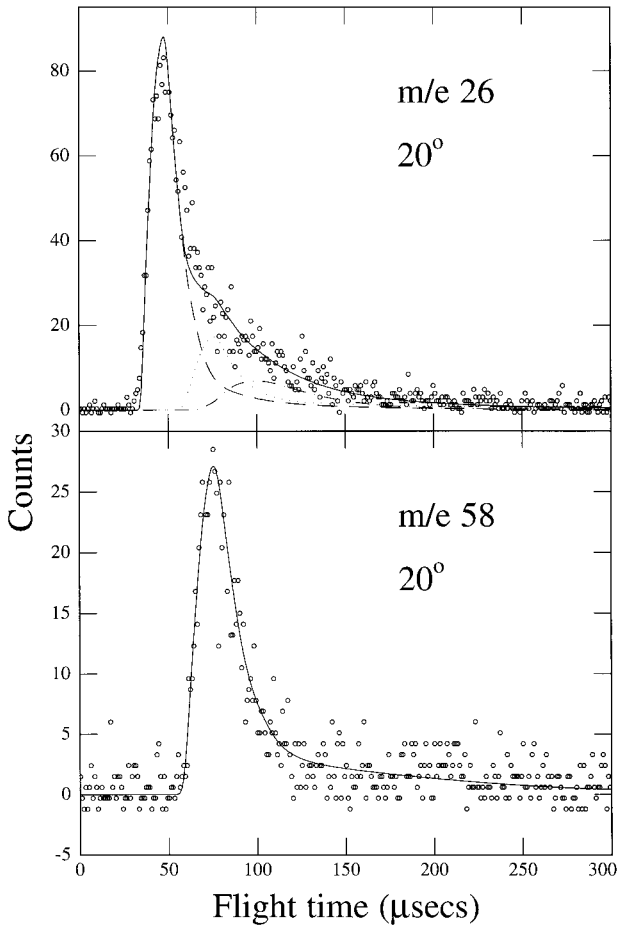

Figure 5. TOF spectra for *m*/*e* 26 and 58 (acetylene and thioketene) at 20°.

for the mass 58 (C_2H_2S) and 26 (C_2H_2), respectively. Figure 5 shows the TOF spectra for the fragments: C_2H_2S and C_2H_2. The translational energy distribution used to fit the TOF spectra for the C_2H_2S fragment is shown in Figure 4. Using this translational energy distribution, the fast part shown in the TOF spectra at mass 26 (C_2H_2) can clearly be momentum matched. The slow part of the C_2H_2 product needs additional contributions to complete the fit. These contributions are from the dissociative ionization of C_4H_4 and C_2H_2S fragments caused by the small amount of higher energy photons. The translational energy distribution (Figure 4) is peaked at 16.2 kcal/mol and extends out to 44.0 kcal/mol, with an average energy release of 19.4 kcal/mol. This result indicates that the C_2H_2 loss channel has a substantial exit barrier.

The energetics for the C_2H_2S + C_2H_2 channel for the different C_2H_2S isomers are[8]

$$C_4H_4S \text{ (thiophene)} + h\nu_{193\text{ nm}} \rightarrow$$

$$H_2C{=}C{=}S + HC{\equiv}CH \qquad \Delta H^0_{298} = -82.0 \text{ kcal/mol} \quad (2a)$$

$$\text{c-HC}{=}\text{CHS} + HC{\equiv}CH \qquad \Delta H^0_{298} \approx -34.0 \text{ kcal/mol} \quad (2b)$$

$$CHCHS + HC{\equiv}CH \qquad \Delta H^0_{298} \approx -20.0 \text{ kcal/mol} \quad (2c)$$

The C_2H_2S fragment is likely thioketene ($H_2C{=}C{=}S$), the more stable of the three isomers according to the following rationale. (1) The onset shown in Figure 2c is at 8.72 eV. This onset is close to the IP (8.77 eV) of thioketene ($H_2C{=}C{=}S$).[13] It is reasonably lower than IP of the thioketene because the C_2H_2S

fragment has significant internal energy. (2) The maximum translational energy distribution occurs at 44.0 kcal/mol and is larger than the available energies of the processes **2b** and **2c**. Hence, thioketene is clearly the dominant, if not the exclusive, C_2H_2S product isomer formed from thiophene dissociation at 193 nm. The analogous channel was observed in furan photodissociation at 193 nm.[2] In the furan study, identity of the C_2H_2O fragment was determined to be ketene ($H_2C{=}C{=}O$). Our result is also consistent with previous studies.[8] Preliminary analysis indicates that channel **2a** occurs on the ground-state potential energy surface following internal conversion. Laser polarization measurements for this channel showed an isotropic angular distribution.

The secondary dissociation processes

$$C_4H_4S\ (\text{thiophene}) + h\nu_{193\ nm} \rightarrow$$
$$CH_2{=}CH{-}C{\equiv}CH + S(^3P) \rightarrow 2HC{\equiv}CH + S(^3P)$$
$$\Delta H^0_{298} \approx 0\ \text{kcal/mol} \quad (2d)$$

$$C_4H_4S\ (\text{thiophene}) + h\nu_{193\ nm} \rightarrow$$
$$H_2C{=}C{=}S + HC{\equiv}CH \rightarrow 2HC{\equiv}CH + S\ (^3P)$$
$$\Delta H^0_{298} \approx 0\ \text{kcal/mol} \quad (2e)$$

are essentially thermoneutral. Although the processes **2d** and **2e** are energetically allowed, the yield will be negligible since it can occur only for the primary products formed with zero translational energy.

The CS + C_3H_4 Channel. This is the weakest of the closed-shell channels. Figure 6 shows TOF spectra of the CS and C_3H_4 fragments obtained at the indicated angles. Photon energies of 12.5 and 10.5 eV were used for measuring the TOF spectra of mass 44 and 40, respectively. In measuring the TOF spectrum of mass 40, the MgF_2 window was used to cut off high-energy scattered radiation, so we need not consider the contribution of larger fragment dissociative ionization. However, a contribution was seen from the stronger radical product at *m*/*e* 39 (C_3H_3) owing to a small amount of mass leakage in the quadrupole. This is seen clearly as the slow component in the bimodal TOF spectrum for *m*/*e* 40 at 20°. The TOF spectra of the CS fragment were also fitted using two components represented by the CS + C_3H_4 channel (a dashed line) and the HCS + C_3H_3 channel (a dash−dot line). Figure 4 shows the P(E) used to fit this channel. The P(E) shows momentum matching between the fast part of mass 40 (C_3H_4) and mass 44 (CS). The P(E) in Figure 4 peaks at 10.0 kcal/mol and extends out to approximately 35 kcal/mol with an average translational energy release of 14.3 kcal/mol. This suggests an exit barrier of at least 10 kcal/mol for this channel.

The C_3H_4 fragment also has different isomers. The dissociations including three energetically allowed structures are listed as follows:

$$C_4H_4S\ (\text{thiophene}) + h\nu_{193\ nm} \rightarrow$$
$$H_3C{-}C{\equiv}CH + CS \qquad \Delta H^0_{298} = -64.3\ \text{kcal/mol} \quad (3a)$$
$$H_2C{=}C{=}CH_2 + CS \qquad \Delta H^0_{298} = -63.0\ \text{kcal/mol} \quad (3b)$$
$$c\text{-}C_3H_4 + CS \qquad \Delta H^0_{298} = -42.3\ \text{kcal/mol} \quad (3c)$$

It is difficult to distinguish which structure is formed in this process judging solely from the reaction energy, since the energetics for **3a** and **3b** are very close. According to the onset

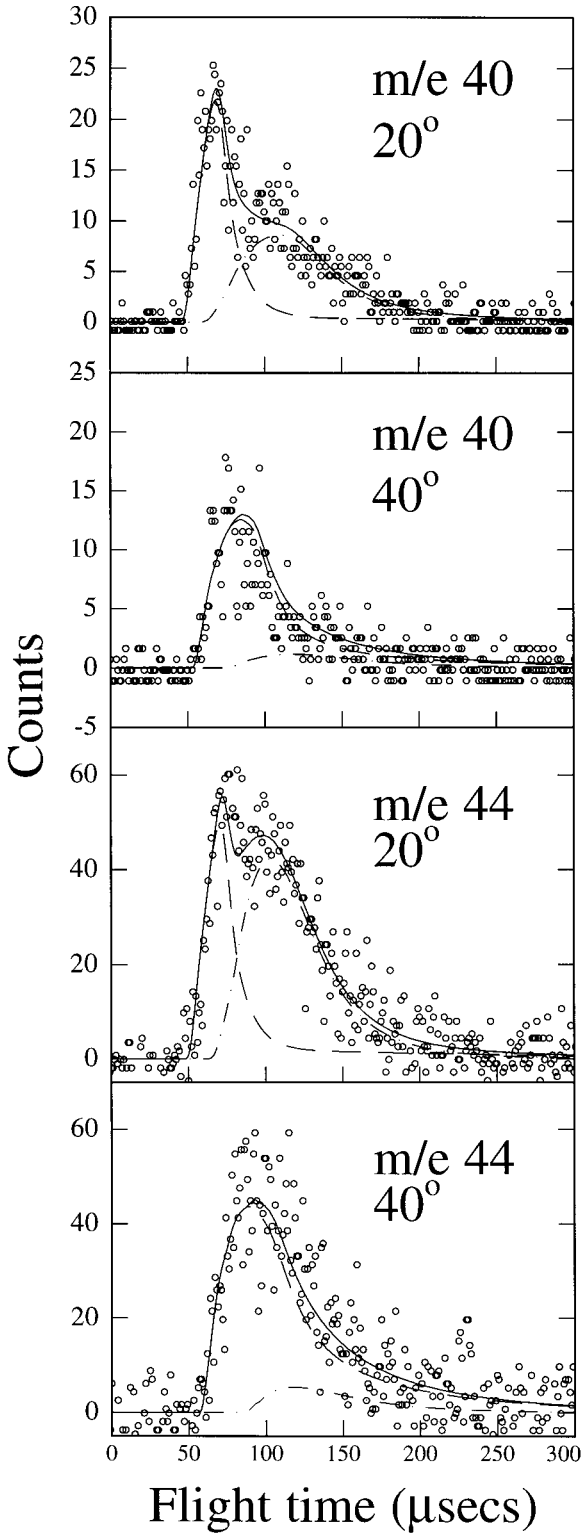

Figure 6. TOF spectra for *m*/*e* 40 and 44 (C_3H_4 and CS) at the indicated laboratory angles.

(9.60 eV) of the C_3H_4 fragment shown in Figure 2d, a closer match to allene ($H_2C{=}C{=}CH_2$, 9.69 eV) than propyne ($H_3C{-}C{\equiv}CH$, 10.37) or cyclopropene (9.67 eV). However, this may still be propyne, with the ionization onset red-shifted by the internal energy. The probability for ring formation is likely to be low, although the IP of cyclopropene is also close to our experimental value. A similar channel was observed at 193 nm photodissociation from furan. However, in the furan case, this was assigned to propyne, largely on the basis of the results of theoretical studies.[15] Similar arguments may well hold for

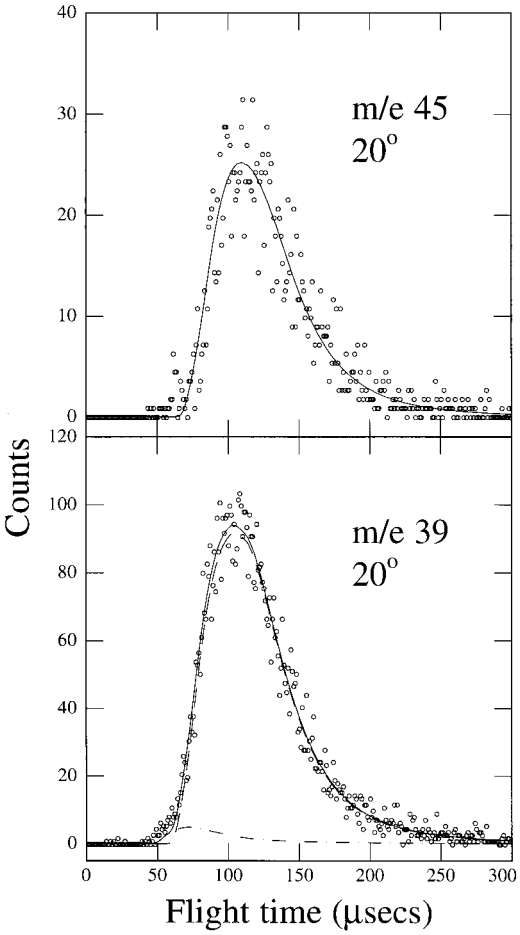

Figure 7. TOF spectra for *m*/*e* 45 and 39 (HCS and C_3H_3) at 20°.

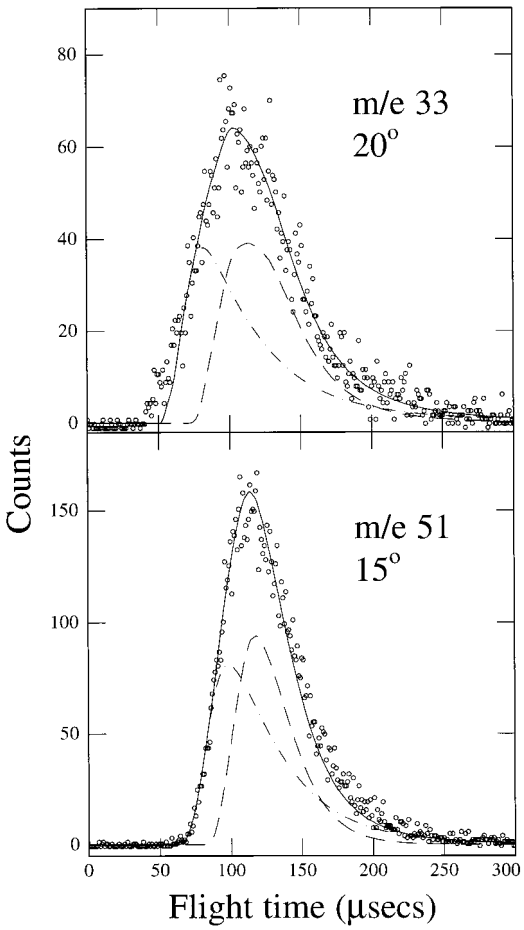

Figure 8. TOF spectra for *m*/*e* 33 and 51 (HS and C_4H_3) at the indicated laboratory angles.

thiophene. The PIE curve (shown in Figure 2f) of the CS fragment was also measured. The onset is around 10.95 eV (IP-(CS): 11.33 eV). A tail was observed at range of 11.2−10.5 eV. This is likely owing to vibrational excitation of the CS fragment.

The HCS + C_3H_3 Channel. Two free radical channels were observed besides the three closed-shell channels mentioned above. The first, HCS + C_3H_3, was seen prominently in furan photodissociation at 193 nm.[2] The TOF spectra of mass 39 (C_3H_3) and mass 45 (HCS) measured at different angles are shown in Figure 7, probed with 9.5 and 10.0 eV photon energies, respectively. A MgF_2 window was used to avoid the dissociative ionization of the C_3H_4 fragment to produce the C_3H_3 ion. The P(E) in Figure 4 was used to fit the HCS + C_3H_3 channel. This P(E) decreases out to about 14.0 kcal/mol with an average translational energy release of 2.9 kcal/mol. The fast part of the TOF spectra of the C_3H_3 fragment have a small contribution on the leading edge that was neither momentum matched to the HCS nor energetically accessible for a one-photon dissociation. It likely represents a small multiphoton contribution. The C_3H_3 fragment was determined to be propargyl radical ($HC{\equiv}C{-}CH_2$), by comparing ionization potentials of the C_3H_3 isomers and the onset shown in the PIE curve (Figure 2b). The formation of cyclopropenyl radical is not allowed energetically. HSC is less stable by 39.6 kcal/mol compared with HCS.[16] The process for forming HSC from thiophene at 193 nm excitation is thus not energetically allowed. We conclude that the mass 45 product is the HCS free radical.

In the 193 nm photodissociation of furan, angular distribution measurements showed anisotropy for the analogous HCO + C_3H_3 channel, indicating that it likely occurs directly on an electronically excited potential energy surface (PES).[2] In contrast, laser polarization measurements for this channel in thiophene show an isotropic angular distribution.

The HS + C_4H_3 Channel. Of all five primary dissociation pathways, the HS + C_4H_3 channel is the weakest one, perhaps due in part to the instability of the C_4H_3 radical. The TOF spectra of mass 33 (HS) and mass 51 (C_4H_3) at different angles are shown in Figure 8. The probe energy was 12.0 and 11.0 eV for ionization of the fragments HS and C_4H_3, respectively. The translational energy distribution shown in Figure 4 was used to fit the HS + C_4H_3 channel. The P(E) peaks near zero and extends out to 7.0 kcal/mol with an average energy release of 1 kcal/mol. The *m*/*e* 51 signal includes a contribution from the stronger *m*/*e* 52 signal. The *m*/*e* 33 fragment also has the contribution of the mass leakage from the much more intense *m*/*e* 32 signal.

An ab initio study of the structures and properties of the free radical C_4H_3 was completed by Ha and Gey.[17] Two low-lying isomers 2-dehydro-buta-1-ene-3-yne (iso-C_4H_3) and 1-dehydro-buta-1-ene-3-yne (*n*-C_4H_3) were found to be the most stable.[17−19] Miller et al. noted that iso-C_4H_3 is thermodynamically more stable (9.6 kcal/mol) than *n*-C_4H_3, and thus most of the C_4H_3 should be in the form of the iso isomer even at combustion temperatures.[20] It seems likely that the C_4H_3 fragment from photodissociation of thiophene survives also as the iso-C_4H_3 isomer ($HC{\equiv}C{-}C{=}CH_2$). The PIE curve of the C_4H_3 fragment is shown in Figure 2e with an onset of about 9.2 eV. No experimental results for the IP of this fragment are available for comparison. Theoretical calculations will be useful for determination of the IP of C_4H_3 isomers. Myers reported one

TABLE 2: Energy Partition of Different Dissociation Channels of Thiophene at 193 nm Excitation (kcal/mol)

dissociation channel (193 nm excitation)	total available energy E_{tot}	max E_{trans}	av E_{trans}	av E_{int}	E_{trans}/E_{int}
$H_2C{=}CH{-}C{\equiv}CH + S(^3P)$	36	17	4.9	31.1	14/86
$H_2C{=}C{=}S + HC{\equiv}CH$	82	44	19.4	62.6	24/76
$H_3C{-}C{\equiv}CH + CS$	64	35	14.3	49.7	22/78
$HCS + HC{\equiv}C{-}CH_2$	23	14	2.9	20.1	13/87
$HS + HC{\equiv}C{-}C{=}CH_2$	26	7	1.0	25.0	4/96

additional channel, giving rise to *m*/*e* 82, that he ascribed predominantly to dimer photodissociation. The absence of signal for *m*/*e* 82 in our experiments provides additional support for this assignment.

Energy Partitioning. From the translational energy distributions of the different channels, the average translational energy release for each channel can be determined. Table 2 lists the obtained maximum translation energies, the average translational energies, the average internal energies, and their ratios for each channel. It is clear that the internal energy partitioning of the photodissociation products from thiophene at 193 nm is always larger than the translational energy release, with the latter ranging from 5% to 24% of the total energy available.

Dissociation Mechanism. Several aspects of the dissociation dynamics in thiophene contrast sharply with the behavior observed for furan. First, the different energetics open the channels to $C_4H_4 + S$ and $C_4H_3 + HS$, for which analogous processes were not seen in furan. More significantly, the $C_3H_3 + HCO$ radical channel which dominates the UV photodissociation of furan is found to be only a minor channel in thiophene. Second, the anisotropy in the photofragment angular distribution for this channel in furan is absent in thiophene. These observations suggest that the competition between direct dissociation on the excited state surface, and internal conversion to the ground state, which was inferred for furan, does not take place in thiophene. Instead, it appears likely that internal conversion to the ground state is rapid, and leads to statistical decomposition of the hot, ground-state molecules. Hsu et al. concluded that the formation of $C_4H_4 + S(^3P)$ could be rationalized by crossing from the upper 2^1B_2 state to the 1^1B_2 state along the dissociation coordinate via nonadiabatic couplings. However, direct dissociation to the 1^1B_2 surface should be very rapid; this is not consistent with the observed angular distributions. In the calculations of Hsu et al., the potential energy surfaces of different excited states were considered only in C_{2v} geometry, i.e., by symmetrically increasing r[S−C(2)] and r[S−C(5)] while keeping other C−C and C−H bond lengths and angles unchanged. The actual dissociation process of excited thiophene clearly involves a change of symmetry from C_{2v} to C_s. In this case, effective coupling exists between all of the A′ surfaces, so that internal conversion directly to the ground state, where the density of states is largest, should be facile. The approximate product yields that we observe are roughly consistent with what one would expect for statistical decomposition to all of the various product channels, given the energetics shown in Figure 1.

The dissociation mechanism of thiophene has not been investigated in detail. Infrared laser multiphoton dissociation[5] and UV photodissociation[8] studies suggested that breakage of the C−S bond in thiophene forms an unstable 1,5-diradical (•CHCHCHCHS•) as the initial step. For the acetylene loss channel, Myers argued that a bond would form between the sulfur atom and C(3), while C(4) and C(5) form the acetylene triple bond and break their bonds with the sulfur atom and C(3). Mass 58 was considered to be thiirene structure in Myers' thesis. However, Hsu et al.[8] and our PIE measurements both indicate that mass 58 is thioketene structure. This suggests that the mechanism proposed by Myers would not explain the acetylene loss channel. Hsu and co-workers also suggested a mechanism that breakage of the C(2)−C(3) and C(4)−C(5) bonds, together with cyclization between C(2) and C(5), would give CH≡CH and c-CH=CHS. The formation of thioketene can be realized if the internal energy content of c-CH=CHS is higher than the rearrangement barrier between c-CH=CHS and CH_2=C=S. The C−S bond strength is weaker than the C=C bond for thiophene. It seems unlikely that two double bonds break and the weaker C−S bond persists. We suspect that scission of the weak C−S bond forms the 1,5-diradical as the initial step, followed by 2,3-H atom migration; the H-atom transfer should be fast because more than 60 kcal/mol average internal energy is available for this channel.

The Acetylene Loss Channel. For the sulfur atom elimination

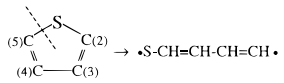

$\rightarrow$ •S-CH=CH-CH=CH•

$\rightarrow$ S=C=CH_2--CH≡CH $\rightarrow$ CH_2=C=S + CH≡CH (2,3-migration)

channel, Myers thought that the closet match for mass 52 would be 3-methylene cyclopropene. One would expect a barrier somewhere along the reaction coordinate for Myers' mechanism since H atom transfer to yield the CH_2 group attached to the ring must occur. In addition, the probability of forming the ring would be small. However, we have shown that mass 58 corresponds to vinyl acetylene, which is in agreement with a previous study.[8] The 1,5-diradical with extensive internal energy could readily undergo bond rearrangement and H atom migration to form vinyl acetylene and sulfur atom.

The Sulfur Atom Elimination Channel. The other three

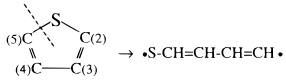

$\rightarrow$ •S-CH=CH-CH=CH•

$\rightarrow$ S--CH≡C-CH=CH_2 $\rightarrow$ S + CH≡C-CH=CH_2 (3,5-migration)

channels would be similar to the two channels discussed above, with formation of the 1,5-diradical as the initial step. The H-atom migration plays an important function in unimolecular decomposition of some other aromatic compounds as well.[15,21−24]

The CS Loss Channel.

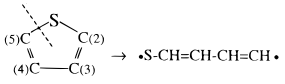

$\rightarrow$ •S-CH=CH-CH=CH•

$\rightarrow$ S-C--H_3C-C≡CH $\rightarrow$ SC+ H_3C-C≡CH (2,3- and 3,4-migrations)

The HCS Loss Channel.

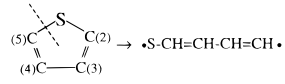

$\rightarrow$ •S-CH=CH-CH=CH•

$\rightarrow$ S-CH--HC≡C-CH_2 $\rightarrow$ HCS+ HC≡C-CH_2 (4,5-migrations)

The HS Loss Channel.

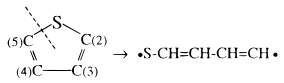

$\rightarrow$ •S-CH=CH-CH=CH•

$\rightarrow$ SH--CH≡C-C=CH_2 $\rightarrow$ HS + HC≡C-C=CH_2 (1,2- and 4,5-migrations)

Thiophene photodissociation is found to be a very complex process. The discussion of dissociation mechanisms above is schematic and based on qualitative arguments and "chemical intuition" according to the identified products. The full elucidation of the detailed mechanism will require theoretical calculations.

IV. Conclusion

We have presented results for the primary photodissociation dynamics of thiophene, c-C_4H_4S 193 nm using tunable synchrotron undulator radiation as a universal product probe. Three closed-shell and two radical channels were identified as primary dissociation processes. Mass 58, 52, 51, 45, 44, 40, 39, 33, 32, and 26 were identified to be thioketene, vinyl acetylene, iso-C_4H_3, HCS radical, CS, allene, propargyl radical, HS, S, and acetylene, respectively. The evidence suggests that dissociation occurs on the ground-state potential surface following internal conversion.

Acknowledgment. This work was supported by the Director, Office of Science, Office of Basic Energy Sciences, Chemical Sciences Division of the U.S. Department of Energy under contract No. DE-AC03-76SF00098. The Advanced Light Source is supported by the Director, Office of Science, Office of Basic Energy Sciences, Materials Sciences Division of the U.S. Department of Energy under the same contract.

References and Notes

(1) Heimann, P. A.; Koike, M.; Hsu, C. W.; Blank, D.; Yang, X. M.; Suits, A. G.; Lee, Y. T.; Evans, M.; Ng, C. Y.; Flaim, C.; Padmore, H. A. *Rev. Sci. Instrum.* **1997**, *68*, 1945.

(2) Sorkhabi, O.; Qi, F.; Rizvi, A.; Suits, A. G. *J. Chem. Phys.* **1999**, 111, 100.

(3) Weissberger, A.; Taylor, E. C.; Gronowitz, S. Thiophene and Its Derivatives. In *The Chemistry of Heterocyclic Compounds*;Wiley: New York, 1992; Vol. 44.

(4) Wiebe, H. A.; Heicklen, J. *Can. J. Chem.* **1969**, *47*, 2965.

(5) Nayak, A. K.; Sarkar, S. K.; Karve, R. S.; Parthasarathy, V.; Rama Rao, K. V. S.; Mittal, J. P.; Krishnamachari, S. L. N. G.; Venkitachalam, T. V. *Appl. Phys. B* **1989**, *B48*, 437.

(6) Krishnamachari, S. L. N. G.; Venkitachalam, T. V. *Chem. Phys. Lett.* **1978**, *55*, 116.

(7) Myers, J. D., Ph.D. Thesis, University of California, 1993.

(8) Hsu, C. W.; Liao, C. L.; Ma, Z. X.; Ng, C. Y. *J. Phys. Chem.* **1995**, *99*, 1760.

(9) Yang, X.; Lin, J.; Lee, Y. T.; Blank, D. A.; Suits, A. G.; Wodtke, A. M. *Rev. Sci. Instrum.* **1997**, *68*, 3317.

(10) Suits, A. G.; Heimann, P.; Yang, X. M.; Evans, M.; Hsu, C. W.; Lu, K. T.; Lee, Y. T.; Kung, A. H. *Rev. Sci. Instrum.* **1995**, *66*, 4841.

(11) Wodtke, A. M., Ph.D. Thesis, University of California at Berkeley, 1986.

(12) Zhao, X., Ph.D. Thesis, University of California at Berkeley, 1988.

(13) Lias, S. G.; Bartmess, J. E.; Liebman, J. F.; Holmes, J. L.; Levin, R. D.; Mallard, W. G. *J. Phys. Chem. Ref. Data* **1988**, *17*, Suppl. 1.

(14) Moore, C. E. *Atomic Energy Levels*; National Bureau of Standards: Washington, D.C., 1949; Vol. I.

(15) Liu, R. F.; Zhou, X. F.; Zhai, L. *J. Comput. Chem.* **1998**, *19*, 240.

(16) Kaiser, R. I.; Sun, W.; Suits, A. G. *J. Chem. Phys.* **1997**, *106*, 5288.

(17) Ha, T. K.; Gey, E. *J.Mol. Struct. (THEOCHEM)* **1994**, *112*, 197.

(18) Kaiser, R. I.; Stranges, D.; Lee, Y. T.; Suits, A. G. *J. Chem. Phys.* **1996**, *105*, 8721.

(19) Walch, S. P. *J. Chem. Phys.* **1995**, *103*, 8544.

(20) Miller, J. A.; Mellius, C. F. *Combust. Flame* **1992**, *91*, 21.

(21) Zhai, L.; Zhou, X.; Liu, R. *J. Phys. Chem. A* **1999**, *103*, 3917.

(22) Lifshitz, A.; Bidani, M.; Bidani, S. *J. Phys. Chem.* **1986**, *90*, 5373.

(23) Lifshitz, A.; Tambura, C.; Shashua, R. *J. Phys. Chem. A* **1997**, *101*, 1018.

(24) Lifshitz, A.; Tambura, C.; Shashua, R. *J. Phys. Chem. A* **1998**, *102*, 10655.

(25) Lide, D. R. *Handbook of Chemistry and Physics*; CRC: Boca Raton, FL, 1995; 75th Ed.

(26) Tsang, W. *Heats of Formation of Organic Free Radicals by Kinetic Methods*; Blackie Academic and Professional: London, 1996.

(27) Kaiser, R. I.; Lee, Y. T.; Suits, A. G. *J. Chem. Phys.* **1996**, *105*, 8705.

(28) Minsek, D. W.; Chen, P. *J. Phys. Chem.* **1990**, *94*, 8399.

(29) Verkoczy, B.; Sherwood, A. G.; Safarik, I.; Strausz, O. P. *Can. J. Chem.* **1983**, *61*, 2268.

(30) Ruscic, B.; Berkowitz, J. *J. Chem. Phys.* **1993**, *98*, 2568.

(31) Kaiser, R. I.; Ochsenfeld, C.; Head-Gordon, M.; Lee, Y. T. *Science* **1998**, *279*, 1181.

(32) Chase, M. W., Jr. *J. Phys. Chem. Ref. Data* **1998**, *9*, 1−1951.

(33) Hsu, C. W.; Baldwin, D. P.; Liao, C. L.; Ng, C. Y. *J. Chem. Phys.* **1994**, *100*, 8047.